



Band tail states and the Anderson transition in amorphous silicon

D.A. Drabold ^{*}, Jianjun Dong

Department of Physics and Astronomy, Condensed Matter and Surface Science Program, Ohio University, Athens, OH 45701-2979, USA

Revised 1 September 1997

Abstract

We compute approximations to the electronic states near the gap in a large and realistic model of a-Si. The spatial structure of the states are computed explicitly and discussed. The properties of the local to extended (Anderson) transition is described. A qualitative picture of the Anderson transition is described. Implications for conductivity and doping are briefly discussed. © 1998 Elsevier Science B.V. All rights reserved.

Keywords: Amorphous silicon; Anderson transition; Conductivity; Doping; Electronic states

1. Introduction

The nature of the band tail states in amorphous semiconductors is of both fundamental and applied interest. Since the seminal work of Anderson [1], it has been known that disorder induces localization of electron states. The detailed understanding of this has been a field of tremendous activity in condensed matter theory. In the parlance of amorphous semiconductors, the nature of the electron localization is determined by the microscopic structure of the band tail and midgap eigenstates and the dependence of this structure on the energy of the state. Here, we report the first explicit microscopic calculations of the band tail states using a very large and realistic 4096 atom model of a-Si (a cube about 4.3 nm on a side), generated by Djordjevic et al. [2]. An orthogonal tight-binding Hamiltonian is used to model the

electron states [3]. While there are important approximations needed where the form of the Hamiltonian is concerned, this paper presents results which are otherwise exact (e.g., with respect to analyzing the spectral properties of the Hamiltonian matrix for the assumed 4096 atom model). A closely related calculation for amorphous diamond has been published recently [4]. To study the nature of electron states in disordered systems, conventional supercell calculations (216 or fewer atoms) are inadequate for any but the most localized (midgap) states. Even in the cell we discuss here, periodic boundary condition artifacts are relevant for states with ‘volume’ comparable to that of the cell.

A localized-to-extended [1] transition is widely believed to occur near both the valence and conduction band tails in a-Si, since it is clear that midgap states are Anderson localized in a realistic model of a-Si and likewise, states well into the valence or conduction bands (beyond the mobility edges) are extended. While this picture is certainly valid, it is also qualitative, and certain details, such as the exact

^{*} Corresponding author. Fax: +1 614 593 0433; e-mail: drabold@helios.phy.ohiou.edu.

structure of the mobility edge are still controversial. Within finite-size limitations of our model, we indicate some features of the transition that are robust and salient to real a-Si, and we suspect are relevant to any topologically disordered system. Perhaps the most interesting feature is that as one considers electron energies varying between midgap and the valence mobility edge, the states become extended by what we will call ‘resonant cluster proliferation’; the electron eigenstates evolve from tightly localized structures with all their weight or ‘charge’ near some major distortion, to weakly coupled ‘droplets’ of charge until ultimately the states fill the volume of the cell, at which point our calculations are unable to draw further conclusions about the properties of the transition since the periodic conditions compel the states to be fully (and artificially) extended.

For applications, and for any transport experiments on a-Si (see, for example, Ref. [5]), the gap and band tail states are of interest. For example, in a Boron doped (p-type) sample of a-Si:H, one can expect that states much like the ones we report near the valence edge will be responsible for the conduction [6]. Any atomistic approach to computing conductivity and transport properties must start from calculations of the electron states near the Fermi level as we compute for a very large cell of a-Si in this paper.

2. Constraints on theory

The approximations of this paper are: (1) an orthogonal tight-binding Hamiltonian [3] with one *s* and three *p* basis functions per site and (2) the 4096 atom supercell model of a-Si proposed in Ref. [2]. The tight-binding model is an imperfect means of modeling electronic structure, but many calculations (see for example, Ref. [7]) demonstrate that the qualitative features of the localization of electronic states due to disorder and their qualitative placement compares well to experiment, or to more sophisticated theory [8]. Computation of forces is another more sensitive matter [9], with which we do not concern ourselves with in this paper. The supercell model of Djordjevic et al. has been discussed in detail in the literature [2]. It has a pair distribution function, bond angle distribution, and as we will

show, electronic properties in rather good and uniform agreement with experiment.

Since the Hamiltonian we are using involves four basis functions per atom, the dimension of the Hamiltonian matrix is $N = 4 \times 4096 = 16384$. This is too large to exactly diagonalize with traditional methods [10]. Since the matrix is sparse (because the range of the tight-binding matrix elements is small), a small subset of the complete set of eigenstates of the matrix can be computed with a Lanczos technique [10]. This approach enables computation of states in a small neighborhood of energy essentially exactly, and its efficiency stems from never requiring operations more computer intensive than the application of the matrix to a vector: matrix multiplications are never required. In a related vein, we use our maximum entropy method [11–14] to compute the global density of states. Both of these approaches can be shown to require both memory and CPU time scaling linearly with *N* (not like N^3 as in full diagonalization methods). A final point is that since the basis set of this Hamiltonian is minimal, we concentrate on the valence tail more than the conduction tail, since the latter is likely to be more affected by the incompleteness of the basis than the valence tail (that is, there is more *s** or *d* character to low-lying conduction states than the valence states).

We estimate the electrical conductivity of the model, using the Kubo formula [15], which is well known and we will not repeat here. By inspection of the Kubo formula, it is clear that the localization of the states, overlap (and momentum matrix elements), and proximity in energy to each other and to the Fermi level, are primary determinants of the DC conductivity. Thermal (electron–phonon) effects are also important at $T > 0$. It is also appropriate to comment that the $\omega \rightarrow 0$ limit of the conductivity is tricky and difficult to unambiguously define for finite systems.

3. Results

Our results are summarized in three figures. The global density of states (DOS) is given in Fig. 1, as obtained by the maximum-entropy method [11–13]. The general shape of the density of states is what we expect of a credible model of a-Si. The gap region is

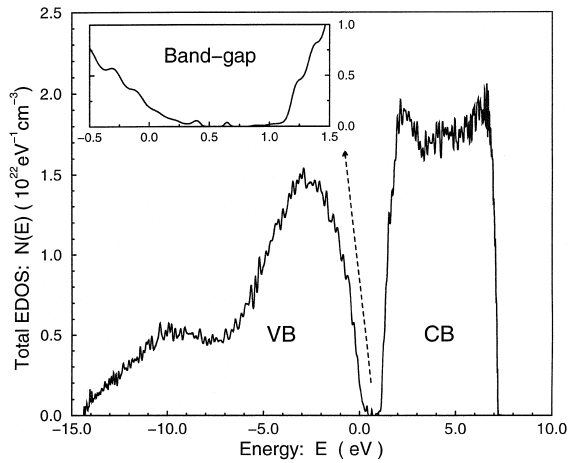


Fig. 1. Total electronic density of states (DOS) of amorphous silicon. Four hundred moments and 50 random vectors were used to achieve the high resolution.

discussed in detail in Fig. 2. In the top panel (Fig. 2a) the position and localization of the states is reported. For each energy for which there is a spike, the Hamiltonian matrix has an eigenvalue. The height of the spike measure the localization using the inverse participation ratio (IPR) [16]. The higher the IPR for a state, the more spatially localized it is. As expected, states near midgap are very localized, and there is a smooth fall off in IPR as energy changes from midgap (say, near 0.5 eV) into the valence tail (near 0.0 eV). The figure emphasizes the essential ambiguity of assigning a ‘valence band edge’ or ‘conduction band edge’. It would seem that the mobility gap extends approximately from 0.0 eV to about 1.2 eV. The structure of the states which are labeled as (a)–(f) is given explicitly in Fig. 3, described below. In Fig. 2b, we reproduce the density of states. Fitting to an exponential fitting function, we estimate that the width of valence band-tail is about 190 meV.

In Fig. 2c, we give an estimate for the zero temperature DC conductivity, where in this plot, the abscissa indicates the position of Fermi level and the predicted conductivity from the states discussed in Fig. 2a. We note that (1) the midgap states are incapable of carrying current, since they are localized and sparse in the energy gap, (2) the states become dense (and extended) enough to give a non-zero conductivity when the model is doped to a

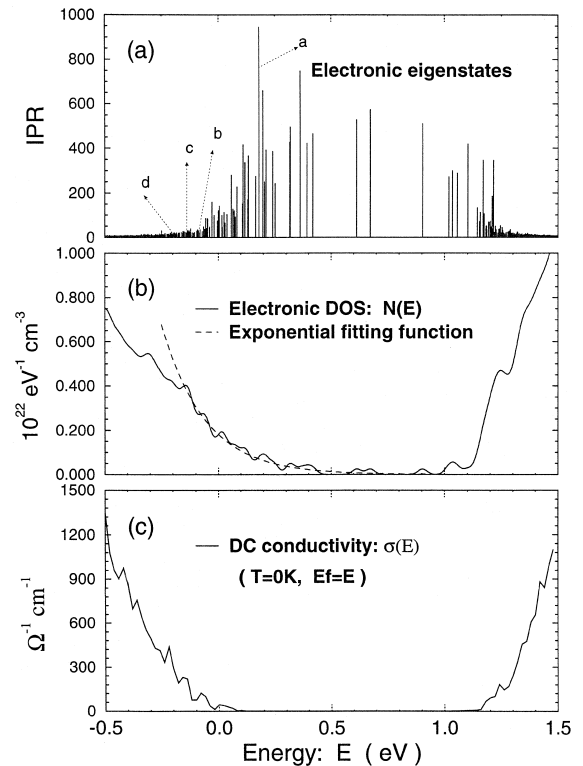


Fig. 2. Electronic states in the band-gap region: (a) Energy and localization, parameterized by inverse participation ratio-IPR, (see text) of electronic eigenstates. The larger the IPR, the more spatially localized the state. The letters illustrate the location in energy of the eigenstates depicted in Fig. 3. (b) Tail DOS. Some localized states tail from the band-edges into band-gap. The valence band-tail is approximately exponential with width of 190 meV as estimated with exponential fitting function (dashed line). (c) The DC conductivity as a function of doping (location of the Fermi level) computed with the Kubo formula. The general shape of the curve is robust; however, the exact onset of a finite DC conductivity depends somewhat on an arbitrary broadening used to evaluate Eq. 3.

Fermi level near $E = 0$, (3) the conductivity rises smoothly with increasing p-doping. There is no evidence in this model of an abrupt mobility edge [17]. The exact location of the mobility edge is difficult to estimate in our theory, because of finite size artifacts. The basic structure of the curve is quite plausible, however. In Fig. 3 we show ‘visualizations’ of the electron states.¹ We show the evolution of states

¹ For a color version, see <http://www.phy.ohiou.edu/~drabold/research.html>.

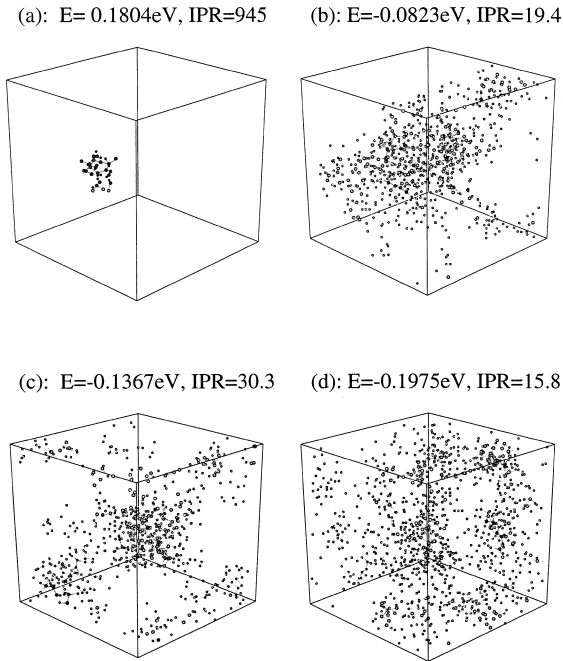


Fig. 3. Spatial character of the local to extended transition. Those atoms which together comprise 75% of the charge of the state are shown. E is energy eigenvalue (the position is also indicated in Fig. 2a). IPR is the inverse participation ratio (see text). The electronic states evolve from highly localized (mid-gap) states (a) into band-tail states (b),(c), and finally to extended valence states (d).

from midgap (Fig. 3a) through the band tail (Fig. 3b,c) to quite extended (Fig. 3d). Note the evolution from a small clump with high charge density (mid-gap, Fig. 3a) to overlapping ‘charge droplets’ roughly in a line (remember that periodic boundary conditions are imposed), to weakly overlapping droplets in Fig. 3c. Fig. 3d shows a quite extended state.

4. Discussion

The most significant outcome of this work is a qualitative understanding of the Anderson transition. In this connection Fig. 3c is particularly revealing, showing that the states become extended by ‘resonant cluster proliferation’ (localization decreases for energies approaching the bandtails by formation of

weakly overlapping droplets). As we argued elsewhere [1], we understand this to be a ‘resonant phenomena’: clusters of atoms with similar energy have their wave functions mixed by small, but non-zero overlap and very small energy denominators. These clusters originate in network irregularities, and would be bona fide eigenstates in their own rights but for other overlapping resonant cluster states. Huge distortions are rare, and are associated with isolated, localized midgap states. Milder distortions are more common, induce less localized states, and have energies closer to the mobility edge. Thus, we find that the volume of the cluster states, and their concentration increases for energies varying between midgap and either mobility edge; at the mobility edge the cluster states sufficiently overlap and the eigenstates become extended [18]. Such a model is sensible only for midgap and tail energies, and is not obviously extendable to the states past either mobility edge.

States such as those illustrated in Fig. 3 are what is needed as input to the Kubo formula [15] and emphasize the complexity of the conductivity, and its dependence on all the details of the electronic eigenstates (and related quantities). In this paper we concentrated on zero temperature, and it is clear that the thermal effects are quite important for the general case. In an adiabatic approximation, the lattice vibrations simply harmonically modulate the positions of the atoms and therefore the electronic states and energies, and the Kubo formula can be thermally averaged to infer an important part of the temperature dependence of the conductivity. Such a study is in progress.

5. Conclusions

We have explored the local-to-extended transition in the most important practical amorphous semiconductor: a-Si. We show that the evolution of the electron states from midgap [local] well into the valence (or conduction) tail [extended] proceeds by ‘cluster proliferation’, as illustrated in Fig. 3. Our work provides a realistic and fairly simple picture of the tail and gap states in amorphous Si.

Acknowledgements

We would like to thank Dr. B.R. Djordjevic and Professor M.F. Thorpe for providing us with their structural model. This work was partially supported by NSF under Grant No. DMR 96-18789 and the Ohio Supercomputer Center under Grant No. PHS218-1.

References

- [1] P.W. Anderson, Phys. Rev. 109 (1958) 1492.
- [2] B.R. Djordjevic, M.F. Thorpe, F. Wooten, Phys. Rev. B 52 (1995) 5685.
- [3] I. Kwon, R. Biswas, C.Z. Wang, K.M. Ho, C.M. Soukoulis, Phys. Rev. B 49 (1994) 7242.
- [4] J. Dong, D.A. Drabold, Phys. Rev. B 54 (1996) 10284.
- [5] G. Adriaenssens, in: M.F. Thorpe, M.I. Mitkova (Eds.), Amorphous Insulators and Semiconductors, NATO ASI Series, Kluwer, Dordrecht, 1997, p. 437.
- [6] P.A. Fedders, D.A. Drabold, Phys. Rev. B 56 (1997) 1864.
- [7] D. Allan, J. Joannopoulos, in: J. Joannopoulos, G. Lucovsky (Eds.), Hydrogenated Amorphous Silicon II, Springer, Berlin, 1984, p. 5.
- [8] O.F. Sankey, D.J. Niklewski, Phys. Rev. B 40 (1989) 3979.
- [9] D.A. Drabold, P.A. Fedders, P. Stumm, Phys. Rev. Lett. 72 (1994) 2666.
- [10] G.H. Golub, C.F. Van Loan, Matrix Computations, Johns Hopkins Univ. Press, Baltimore, 1983.
- [11] D.A. Drabold, O.F. Sankey, Phys. Rev. Lett. 70 (1993) 3631.
- [12] D.A. Drabold, in: M.F. Thorpe, M.I. Mitkova (Eds.), Amorphous Insulators and Semiconductors, NATO ASI Series, Kluwer, Dordrecht, 1997, p. 405.
- [13] D.A. Drabold, P. Ordejón, J. Dong, R.M. Martin, Solid State Commun. 96 (1995) 833.
- [14] P. Ordejón, D.A. Drabold, R.M. Martin, Phys. Rev. Lett. 75 (1995) 1324.
- [15] D.J. Thouless, Phys. Rep. 13 (1974) 93.
- [16] J. Ziman, Models of Disorder, Cambridge Univ. Press, Cambridge, 1979.
- [17] N.F. Mott, E.A. Davis, Electronic Processes in Non-Crystalline Materials, 2nd edn., Clarendon Press, Oxford, 1979.
- [18] J. Dong, D.A. Drabold, Phys. Rev. Lett. 80 (1998) 1928.